N76-21059

SPECTROSCOPIC OBSERVATIONS OF COMET KOHOUTEK (1973f)

Lubos Kohoutek and Jurgen Rahe

1. Introduction

Between January 5 and January 15, 1974, nine coudé spectrograms of Comet Kohoutek (1973f) were obtained with the ESO 152-cm telescope in La Silla, Chile. The emulsion is Kodak IIa-O (3 plates) and Kodak 103a-F (6 plates), the dispersion is 20.2 Å/mm. The useful spectral range extends from about 3500 Å to about 5000 Å (Kodak IIa-O plates) and from about 4500 Å to about 6700 Å (Kodak 103a-F plates). The original scale was 4.55 arc sec/mm on the slit, and the full length of the slit was about 3 arc minutes. 1 mm on the plates corresponds to 66.5 arc sec, or about $3.9 - 4.4 \times 10^4$ km at the Comet projected on the plane of the sky. The slit was always centered on the image of the Comet, and except for plate No. 1436, was oriented along the radius vector. A field rotator was used which dimished the stellar light by about 30 %.

During the time of observation the heliocentric distance, r and the geocentric distance, Δ of the Comet varied from

$$r = 0.34 - 0.63 \text{ AU}$$

$$\Delta = 0.92 - 0.81 \text{ AU}.$$

The pertinent observational and cometary data are given in Table 1. All observations were severely influenced by large extinction.

Table 1
Spectroscopic Observations of Comet Kohoutek (1973f)

Plate No.	Date U.T. (1974)	Emulsion (Kodak)	Quality	Exposure (min.)	α(Comet) 1950	δ(Comet) 1950	r (AU)	Δ(AU)	$d\Delta/dt$ (Km/sec)
1436	Jan. 5.025	103a-F	weak	11	$20^h\ 20^m.8$	$-15^\circ\ 51'$	0.338	0.916	-37.44
1439	Jan. 6.025	103a-F	good	30	20 32.7	-15 02	0.369	0.897	-33.54
1445	Jan. 7.031	103a-F	weak	30	20 44.6	-14 12	0.401	0.877	-29.66
1452	Jan. 8.030	103a-F	weak	37	20 56.4	-13 21	0.431	0.863	-25.89
1459	Jan. 9.033	IIa-0	weak	25	21 08.2	-12 28	0.462	0.847	-22.16
1470	Jan. 10.035	IIa-0	good	42	21 19.9	-11 34	0.491	0.837	-18.54
1478	Jan. 12.036	103a-F	weak	54	21 43.3	- 9 41	0.549	0.819	-11.45
1501	Jan. 14.040	IIa-0	good	56	22 06.3	- 7 45	0.604	0.810	- 4.69
1503	Jan. 15.040	103a-F	weak	58	22 17.6	- 6 46	0.631	0.807	- 1.45

2. Blue Region of the Spectrum

In the Kodak IIa-O plates, the violet system of CN and the C_2 Swan bands are dominating. In addition we find emission features of the C_3, CH, and CO^+ molecules. The (0-0) and the (0-1) bands of the ($B^2\Sigma - X^2\Sigma$) system of CN are well resolved. On plate No. 1501, the (0-0) band could be traced up to R(26). The much fainter (1-1) band could not be detected. Tables 2 and 3 contain the wavelengths measured and corrected for the Doppler shift due to the geocentric radial velocity of the Comet, the visual estimates of the corresponding intensities on an arbitrary scale, and the identifications. The identifications in these and the following tables are based on Johnson (1927), Shea (1927), Phillips (1948), Hunaerts (1950), Weinard (1955), Dressler and Ramsay (1959), Dossin et al. (1961), and Greenstein and Arpigny (1962).

The $\Delta v = +1$ sequence of the C_2 Swan bands ($A^3\Pi - X^3\Pi$) can easily be recognized. Of C_3 only three emissions could be found: λ4039.56 Å (I=1), λ4043.42 Å (2), λ4051.71 Å (4). The (0-0) bands of the ($B^2\Sigma - X^2\Pi$) and the ($A^2\Delta - X^2\Pi$) systems of CH are present, the latter, however, always much stronger than the first which shows essentially the $P_1(1)$ λ3892.93 emission. Table 4 lists the identified CH emissions of the (0-0) band of the ($A^2\Delta - X^2\Pi$) system. CO^+ is present only in the best IIa-O plate (No. 1501) with

Table 2
The (0-0) Band of the $B^2\Sigma$ - $X^2\Sigma$ System of CN

Intensity	λ (Å) (observed)	Identification λ (Lab)
1	3852.32	R(26) 3852.41
0	3853.35	R(25) 3853.50
2	3855.66	R(23) 3855.63
1	3856.44	R(22) 3856.67
3	3857.65	R(21) 3857.68
3	3858.67	R(20) 3858.64
4	3859.67	R(19) 3859.67
1	3860.58	R(18) 3860.60
2	3861.52	R(17) 3861.54
6	3862.40	R(16) 3862.48
9	3863.31	R(15) 3863.40
6	3864.23	R(14) 3864.30
9	3865.08	R(13) 3865.16
6	3865.91	R(12) 3865.99
10	3866.75	R(11) 3866.82
8	3867.61	R(10) 3867.62
8	3868.36	R(9) 3868.41
11	3869.05	R(8) 3869.18
9	3869.82	R(7) 3869.92
1	3870.58	R(6) 3870.65
3	3871.25	R(5) 3871.37
6	3872.03	R(4) 3872.05
3	3872.62	R(3) 3872.74
5	3873.29	R(2) 3873.37
5	3873.98	R(1) 3874.00
0	3874.61	R(0) 3874.61
0n	3875.84	P(2) 3876.32
3	3876.70	P(3) 3876.84
2	3877.20	P(4) 3877.35
1	3877.41	P(5) 3877.84
6n	3881.05	P(13) 3880.99
6n	3882.05	P(14) 3881.30 P(15) 3881.58
6n	3882.99	Head 3883.39

Table 3
The (0-1) Band of the $B^2\Sigma - X^2\Sigma$ System of CN

Intensity	λ (Å) (observed)	Identification λ (Lab)
1	4195.97	R(13) 4195.94
1	4198.02	R(11) 4198.09
0	4206.02	R(2) 4206.19
1	4207.04	R(1) 4206.95
1	4211.85	P(6) 4211.90
3	4215.60 Head	P(17) 4215.55 P(18) 4215.68

Table 4
The (0-0) Band of the $A^2\Delta$ - $X^2\Pi$ System of CH

Intensity	λ (Å) (observed)	Identification λ (Lab)
3	4291.06	$R_2cd(3)$ 4291.11, $R_2dc(3)$ 4291.22
2	4292.08	$R_1cd(3)$ 4292.05, $R_1dc(3)$ 4292.12
5	4296.60	$R_2cd(2)$ 4296.62, $R_2dc(2)$ 4296.66
5	4297.95	$R_1cd(2)$ 4297.99, $R_1dc(2)$ 4297.99
4	4300.31	$R_2cd(1)$ 4300.32, $R_2dc(1)$ 4300.32
10	4303.88	$R_1cd(1)$ 4303.95, $R_1dc(1)$ 4303.95
9	4312.64	$Q_2d(3)$ 4312.59, $Q_2d(2)+Q_2c(2)$ $+Q_2c(3)$ 4312.71
9	4314.11	$Q_1c(2)$ 4314.21, $Q_1d(2)$ 4314.21
2	4329.97	$P_1cd(3)$ 4329.94, $P_1dc(3)$ 4330.00
2	4334.01	$P_2cd(4)$ 4333.84, $P_2dc(4)$ 4334.00, $P_1cd(4)$ 4334.66, $P_1dc(4)$ 4334.78
2n	4338.74	$P_2cd(5)$ 4338.63, $P_2dc(5)$ 4338.85

Table 5
CO^+ Bands

$(v' - v'')$	λ (Å)	System	
(1-0)	4568 - 4544	$A^2\Pi$ - $X^2\Sigma$	Comet Tail
(2-0)	4252	$A^2\Pi$ - $X^2\Sigma$	Comet Tail
(2-1)	4711 - 4683	$A^2\Pi$ - $X^2\Sigma$	Comet Tail
(0-1)	4231	$B^2\Sigma$ - $X^2\Pi$	Baldet-Johnson

Table 6
Emissions in the Visual Region of the Spectrum

Intensity	λ (Å) (observed)	Identification
8	4684.35	$C_2(4-3)$ Head
10	4696.65	$C_2(3-2)$ Head
5	4704.97	$C_2(2-1)$ $P_1(40)$, $P_2(39)$
8	4714.32	$C_2(2-1)$ Head
10	4736.60	$C_2(1-0)$ Head
3n	4941.83	$C_2(0-0)$ $R_1(72)$, $R_2(71)$, $R_3(70)$
2	4967.46	$C_2(1-1)$ $R_3(58)$, $R_1(60)$, $R_2(59)$
		$C_2(0-0)$ $P_3(93)$
1	4970.00	$C_2(0-0)$ $R_1(66)$, $R_2(65)$, $R_3(64)$
1	4992.37	$C_2(0-0)$ $R_3(59)$, $R_1(61)$, $R_2(60)$
2	4996.69	$C_2(0-0)$ $R_1(60)$, $R_2(59)$, $R_3(58)$
2	5005.42	$C_2(0-0)$ $R_3(56)$, $R_1(58)$, $R_2(57)$
3	5009.50	$C_2(0-0)$ $R_3(55)$, $R_1(57)$, $R_2(56)$
		$C_2(1-1)$ $R_1(49)$, $R_2(48)$
1	5013.58	$C_2(0-0)$ $R_3(54)$, $R_1(56)$, $R_2(55)$
1	5017.53	$C_2(0-0)$ $R_1(55)$, $R_2(54)$
2	5021.88	$C_2(0-0)$ $R_1(54)$, $R_2(53)$, $R_3(52)$
3	5033.83	$C_2(0-0)$ $R_3(49)$, $R_1(51)$, $R_2(50)$
		$C_2(1-1)$ $R_3(40)$, $R_1(42)$, $R_1(41)$
1	5037.69	$C_2(0-0)$ $R_3(48)$, $R_1(50)$, $R_2(49)$
1	5052.70	$C_2(0-0)$ $R_3(44)$, $R_1(46)$, $R_2(45)$
		$C_2(1-1)$ $R_1(36)$, $R_2(35)$, $R_3(34)$
3	5055.95	$C_2(0-0)$ $R_1(45)$, $R_2(44)$, $R_3(43)$
		$C_2(1-1)$ $R_3(33)$, $R_2(34)$, $R_1(35)$
3	5063.13	$C_2(0-0)$ $R_1(43)$, $R_2(42)$, $R_3(41)$
3	5069.95	$C_2(0-0)$ $R_3(39)$, $R_1(41)$, $R_2(40)$
		$C_2(2-2)$ $R_1(16)$, $R_2(15)$
2	5073.38	$C_2(0-0)$ $R_1(40)$, $R_2(39)$, $R_3(38)$
		$C_2(2-2)$ $R_1(14)$, $R_2(13)$
3	5083.00	$C_2(0-0)$ $R_1(37)$, $R_2(36)$, $R_3(35)$
2	5086.25	$C_2(0-0)$ $R_3(34)$, $R_1(36)$, $R_2(35)$
		$C_2(1-1)$ $R_1(23)$, $R_2(22)$
3	5089.10	$C_2(0-0)$ $R_1(35)$, $R_2(34)$
		$C_2(1-1)$ $R_1(22)$, $R_2(21)$
4	5092.24	$C_2(0-0)$ $R_1(34)$, $R_2(33)$, $R_3(32)$
1	5095.35	$C_2(0-0)$ $R_3(31)$, $R_1(33)$, $R_2(32)$
		$C_2(1-1)$ $R_1(19)$, $R_2(18)$,
1	5097.06	$C_2(2-2)$ Head $P_3(17)$, $P_1(18)$, $P_1(17)$, $P_1(19)$, $P_2(18)$, $P_3(18)$

Table 6 (Continued)

Intensity	λ (Å) (observed)	Identification	
2	5100.84	C_2 (0-0)	$R_3(29)$, $R_2(30)$, $R_1(31)$
		C_2 (1-1)	$R_1(16)$, $R_2(15)$
3	5103.71	C_2 (0-0)	$R_1(30)$, $R_2(29)$, $R_3(28)$
		C_2 (1-1)	$P_3(42)$, $P_1(44)$, $P_2(43)$
1	5106.40	C_2 (0-0)	$R_1(29)$, $R_2(28)$, $R_3(27)$
2	5111.60	C_2 (0-0)	$R_1(27)$, $R_2(26)$, $R_3(25)$
1	5113.00	C_2 (1-1)	$P_1(38)$, $P_2(37)$, $P_3(36)$
		C_2 (0-0)	$P_1(55)$, $P_2(54)$
1	5116.75	C_2 (0-0)	$R_1(25)$, $R_2(24)$, $R_3(23)$
		C_2 (1-1)	$P_1(35)$, $P_2(34)$, $P_3(33)$
1	5120.54	C_2 (1-1)	$P_3(30)$, $P_1(32)$, $P_2(31)$
		C_2 (0-0)	$P_1(52)$, $P_2(51)$, $P_3(50)$
1	5121.30	C_2 (0-0)	$R_1(23)$, $R_2(22)$
7	5128.70	C_2 (1-1)	Head $P_1(21)$, $P_2(20)$, $P_3(19)$
2	5141.46	C_2 (0-0)	$P_3(40)$, $P_1(42)$, $P_2(41)$, $R_1(13)$
3	5144.54	C_2 (0-0)	$P_3(38)$, $P_1(40)$, $P_2(39)$
2	5146.15	C_2 (0-0)	$P_1(39)$, $P_2(38)$, $P_3(37)$
1	5147.73	C_2 (0-0)	$P_3(36)$, $P_1(38)$, $P_2(37)$
3	5149.11	C_2 (0-0)	$P_3(35)$, $P_1(37)$, $P_2(36)$, $R_1(8)$
1	5150.49	C_2 (0-0)	$P_1(36)$, $P_2(35)$, $P_3(34)$
2	5155.58	C_2 (0-0)	$P_1(32)$, $P_2(31)$, $P_3(30)$
1	5157.78	C_2 (0-0)	$P_1(30)$, $P_2(29)$, $P_3(28)$
1	5158.49	C_2 (0-0)	$P_1(29)$, $P_2(28)$, $P_3(27)$

Table 6 (Continued)

Intensity	λ (Å) (observed)	Identification	
20	5164.81	C_2 (0-0)	Head $P_3(18)$, $P_1(19)$, $P_2(18)$, $P_1(18)$, $P_2(17)$, $P_3(16)$
1n	5409.09	$NH_2(1,7,0)$	$2_{02}-3_{12}$
4	5428.60	$NH_2(0,11,0)$	$2_{02}-2_{12}$, $4_{04}-4_{14}$, $3_{03}-3_{13}$, $1_{01}-1_{11}$
2	5441.12	C_2 (0-1)	$P_1(81)$, $P_2(80)$
3	5442.81	$NH_2(1,7,0)$	$2_{21}-1_{11}$
3	5451.80	C_2 (0-1)	$R_1(54)$, $P_1(79)$, $P_2(78)$
		C_2 (1-2)	$R_3(43)$, $R_1(45)$, $R_2(44)$
3	5472.55	C_2 (3-4)	$R_3(13)$, $R_2(14)$, $R_1(15)$
		C_2 (2-3)	$R_1(29)$, $R_2(28)$, $R_3(27)$
		C_2 (0-1)	$R_1(50)$, $R_2(49)$, $R_3(48)$, $P_1(75)$, $P_2(74)$
1	5485.40	C_2 (1-2)	$R_1(37)$, $R_2(36)$, $R_3(35)$
2n	5492.34	C_2 (0-1)	$R_3(44)$, $R_1(46)$, $R_2(45)$, $P_1(71)$, $P_2(70)$
2n	5496.91	C_2 (0-1)	$R_3(43)$, $R_1(45)$, $R_2(44)$, $P_1(70)$, $P_2(69)$
		C_2 (1-2)	$R_1(34)$, $R_2(33)$,
5	5501.43	C_2 (3-4)	Head
		C_2 (2-3)	$R_3(17)$, $R_2(18)$
		C_2 (0-1)	$R_1(44)$, $R_2(43)$, $P_1(69)$, $P_2(68)$
2	5505.96	C_2 (0-1)	$R_3(41)$, $P_1(68)$, $P_2(67)$, $R_1(43)$, $R_2(42)$
		C_2 (2-3)	$R_3(15)$
2	5514.81	C_2 (0-1)	$R_1(41)$, $R_2(40)$, $R_3(39)$
		C_2 (1-2)	$R_2(29)$, $R_2(28)$, $R_3(27)$
		C_2 (2-3)	$R_3(11)$
3	5523.78	C_2 (0-1)	$R_3(37)$, $R_1(39)$, $R_2(38)$, $P_1(64)$, $P_2(63)$
2	5527.78	C_2 (0-1)	$R_1(38)$, $R_2(37)$, $R_3(36)$, $P_1(63)$, $P_2(62)$, $P_3(61)$
		C_2 (1-2)	$R_3(23)$, $R_2(24)$, $R_1(25)$
3	5532.11	C_2 (0-1)	$R_3(35)$, $R_1(37)$, $R_2(36)$

Table 6 (Continued)

Intensity	λ (Å) (observed)	Identification	
3	5536.26	C_2 (0-1)	$R_3(34)$, $P_1(61)$, $P_2(60)$, $R_1(36)$, $R_2(35)$
1	5537.52	C_2 (2-3)	$P_3(20)$, $P_1(22)$, $P_2(21)$
4	5540.20	C_2 (2-3)	Head $P_3(17)$, $P_1(18)$, $P_2(17)$, $P_2(16)$, $P_3(16$
			$P_3(15)$, $P_2(15)$, $P_2(14)$, $P_3(14)$, $P_2(13)$
2	5544.04	C_2 (0-1)	$R_1(34)$, $R_2(33)$, $R_3(32)$, $P_1(59)$,
			$P_2(58)$
2	5551.54	C_2 (0-1)	$R_2(32)$, $R_2(31)$, $R_3(30)$, $P_1(57)$, $P_2(56)$
2	5559.10	C_2 (0-1)	$R_3(28)$, $P_1(55)$, $P_2(54)$, $P_3(53)$
3	5565.68	C_2 (0-1)	$R_1(28)$, $R_2(27)$, $R_3(26)$, $P_1(53)$, $P_2(52)$
		C_2 (1-2)	$P_3(33)$, $P_1(35)$
1	5569.20	C_2 (0-1)	$R_2(26)$, $R_3(25)$, $R_1(27)$
		C_2 (1-2)	$P_3(31)$
2	5572.38	C_2 (0-1)	$R_1(26)$, $R_2(25)$
		C_2 (1-2)	$P_3(29)$, $P_1(31)$, $P_2(30)$
10	5585.02	C_2 (1-2)	Head $P_1(18)$, $P_2(17)$, $P_3(16)$, $P_1(17)$,
			$P_2(16)$, $P_3(15)$, $P_1(16)$, $P_2(15)$, $P_1(15)$,
			$P_2(14)$, $P_3(14)$, $P_1(14)$, $P_2(13)$
		C_2 (0-1)	$R_1(22)$, $R_2(21)$, $R_3(20)$, $P_1(47)$, $P_2(46)$
1n	5588.07	C_2 (0-1)	$P_1(46)$, $P_2(45)$, $P_3(44)$
1	5590.70	C_2 (0-1)	$R_3(18)$, $P_1(45)$, $P_2(44)$, $R_2(19)$
1	5593.55	C_2 (0-1)	$R_3(17)$, $P_1(44)$, $P_2(43)$, $P_3(42)$
		$NH_2(0,11,0)$	$5_{41}-4_{31}$
1	5595.99	C_2 (0-1)	$R_1(18)$, $R_2(17)$, $R_3(16)$, $P_1(43)$, $P_2(42)$
2	5600.72	C_2 (0-1)	$R_1(16)$, $R_2(15)$, $R_3(14)$, $P_1(41)$, $P_2(40)$
1n	5612.33	C_2 (0-1)	$P_1(36)$, $P_2(35)$, $P_3(34)$
1n	5614.27	C_2 (0-1)	$P_1(35)$, $P_2(34)$, $P_3(33)$

C. 3

Table 6 (Continued)

Intensity	λ (Å) (observed)	Identification	
6	5635.06	C_2 (0-1)	Head $P_3(14)$, $P_3(15)$, $P_1(17)$, $P_2(16)$, $P_3(16)$
2	5703.06	$NH_2(0,10,0)$	$2_{12}-2_{02}$
30	5889.92	Na I	D_2
20	5895.89	Na I	D_1
1	5939.47	$NH_2(0,10,0)$	$5_{32}-6_{42}$
6	5977.02	C_2 (3-5)	$R_2(11)$, $R_1(12)$
		$NH_2(0,9,0)$	$3_{03}-3_{13}$, $5_{05}-5_{15}$, $1_{01}-1_{11}$, $2_{02}-2_{12}$
5	5994.96	$NH_2(0,9,0)$	$1_{01}-2_{11}$
		C_2 (1-3)	$R_1(37)$, $R_2(36)$, $R_3(35)$
		C_2 (3-5)	$P_1(26)$, $P_2(25)$
3	6004.21	C_2 (3-5)	Head
		$NH_2(0,9,0)$	$4_{23}-3_{13}$
5	6020.03	$NH_2(0,9,0)$	$3_{03}-4_{13}$
		C_2 (1-3)	$R_2(31)$, $R_3(30)$
3	6033.56	C_2 (1-3)	$R_1(29)$, $R_2(28)$, $R_3(27)$
		C_2 (2-4)	$P_1(34)$, $P_2(33)$
		$NH_2(0,9,0)$	$3_{21}-3_{13}$
3n	6059.14	C_2 (2-4)	Head
1	6081.51	$NH_2(0,9,0)$	$4_{23}-4_{31}$
1	6096.71	$NH_2(0,9,0)$	$2_{21}-3_{31}$, $2_{20}-3_{30}$
2	6098.44	$NH_2(0,9,0)$	$2_{20}-3_{30}$, $2_{21}-3_{31}$
3	6121.86	C_2 (1-3)	Head
2	6190.74	C_2 (0-2)	Head

Table 6 (Continued)

Intensity	λ (Å) (observed)	Identification
1	6255.89	$NH_2(0,9,0)$ $6_{43}-6_{33}$
1	6274.28	$NH_2(0,8,0)$ $3_{12}-2_{02}$
1	6297.32	$NH_2(0,8,0)$ $2_{12}-2_{02}$
2	6298.58	$NH_2(0,8,0)$ $2_{12}-2_{02}$
10	6300.33	$NH_2(0,8,0)$ $4_{14}-4_{04}$, $6_{16}-6_{06}$ [OI]
3	6334.56	NH_2(Em)
1	6357.46	$NH_2(0,8,0)$ $3_{13}-4_{23}$
2	6360.31	$NH_2(0,8,0)$ $3_{12}-4_{22}$
2	6363.87	[OI]
1	6601.40	$NH_2(0,7,0)$ $3_{03}-2_{11}$, $4_{04}-3_{12}$, $5_{05}-4_{13}$
1	6618.07	$NH_2(0,7,0)$ $1_{01}-1_{11}$
2	6619.08	$NH_2(0,7,0)$ $5_{05}-5_{15}$, $3_{03}-3_{13}$, $2_{02}-2_{12}$
2	6640.62	$NH_2(0,7,0)$ $1_{01}-2_{11}$
2	6671.47	$NH_2(0,7,0)$ $3_{03}-4_{13}$

its emissions given in Table 5. It was too faint to be seen in any other spectrum.

3. Visual Region of the Spectrum

Table 6 contains the list of the measured emissions in the visual region of the spectrum with wavelengths λλ4684-6671 Å (Kodak 103a-F plates) together with the corresponding identifications. We find essentially the sequences $\Delta v = 0$, $\Delta v = -1$, and $\Delta v = -2$ of the C_2 Swan bands, and NH_2 emissions. Since NH_2 is more concentrated towards the nucleus than C_2, it is easier lost in the continuum than C_2. In addition to C_2 and NH_2, the NaI D_1 and D_2 lines are very strong, and forbidden [OI] can also be identified. New lines could not be detected.

4. Discussion

The sodium doublet (5889.97 Å, 5895.93 Å) was very strong at small heliocentric distances (0.3 - 0.4 AU), but later it weakened considerably. The intensity distribution along the lines is given in Figures 1 and 2. The profiles are remarkably asymmetric with respect to the nucleus; the gradient on the sunward side (S) is much steaper than on the tail side (RV). The intensity decrease of Na in the nucleocentric distance between 2 and 5×10^3 km on the sunward side and between 2 and 7×10^3 km on the tail side is approximately linear with a mean slope of -20 and -12, respectively. Towards the sun, Na extends to about 1.2×10^4 km,

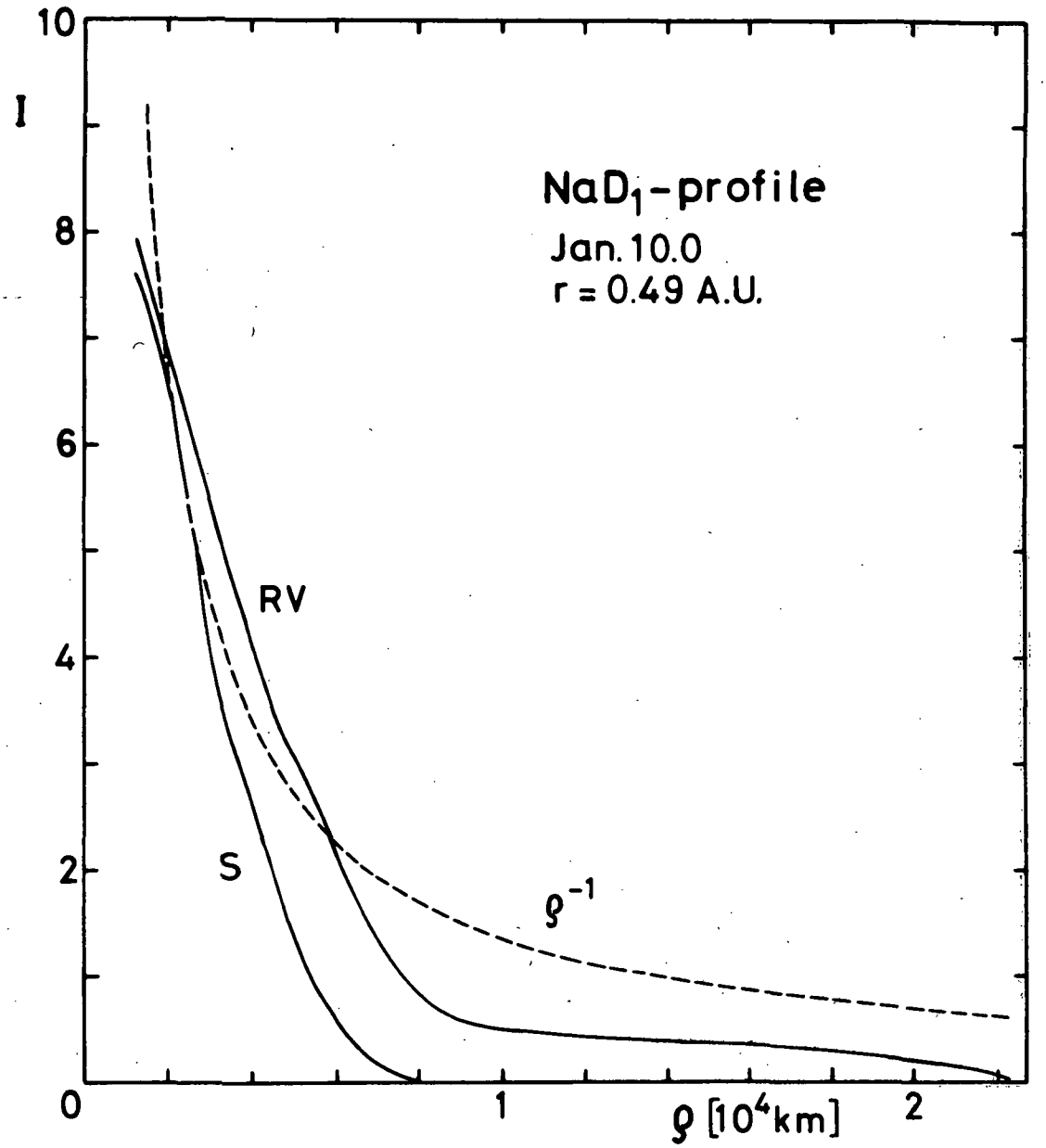

Figure 1: Na D_1-profile on January 10.035 UT, 1974, at r = 0.49 AU. The intensity (I) is given in arbitrary units as function of the distance (ρ) from the nucleus in units of 10^4 km in the direction towards the sun, (S); and in the tail direction, (RV). The dashed curve is calculated for an intensity law $I(\rho) \sim \rho^{-1}$.

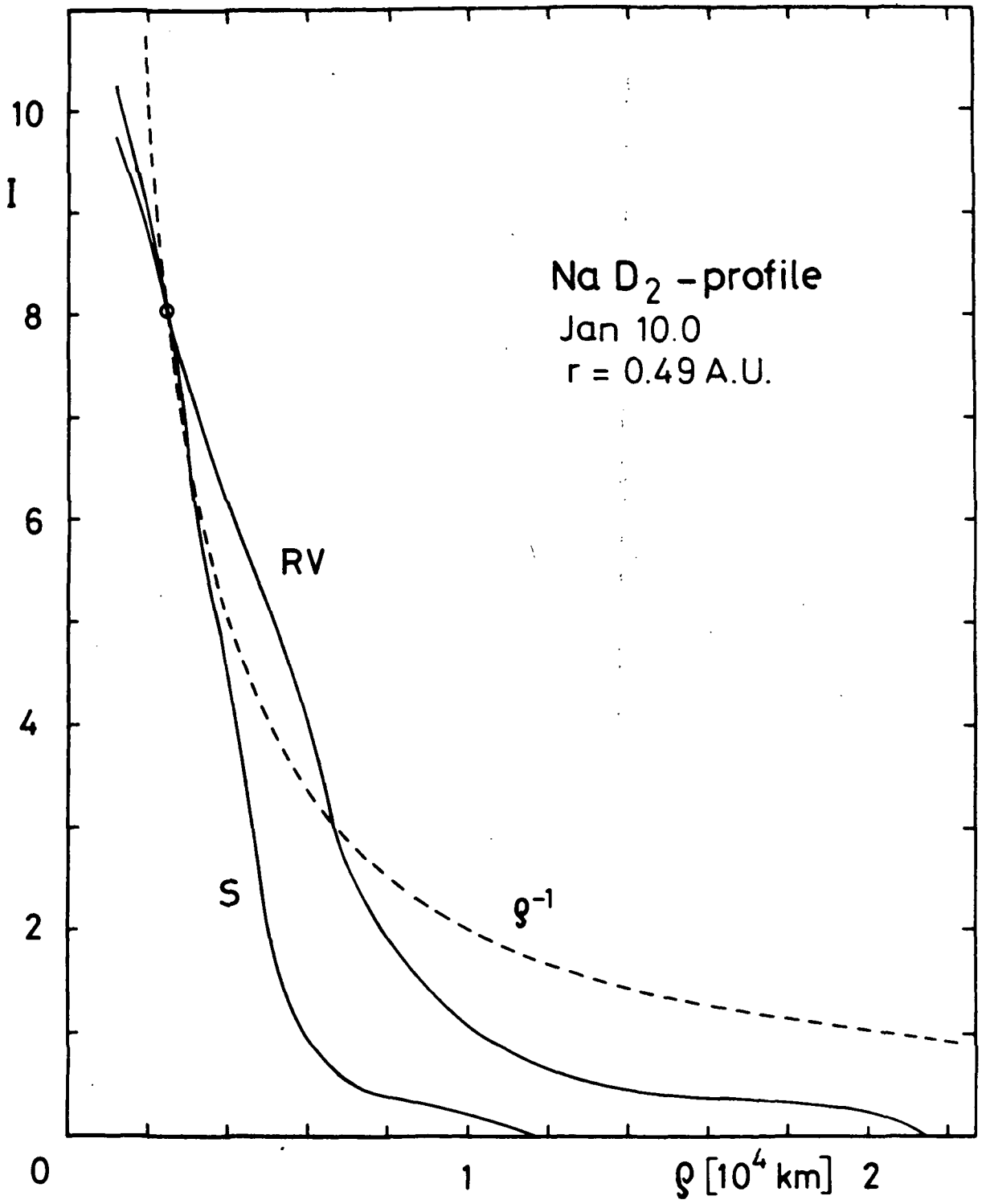

Figure 2: Na D_2-profile on January 10.035 UT, 1974, at r = 0.49 AU. For details see Fig. 1.

in the tail direction up to over 2×10^4 km. This asymmetry is caused by radiation pressure. Due to their larger f-values, the Na D-lines are more sensitive to this effect than the neutral molecular emissions ($f(CN) = 3 \times 10^{-2}$, $f(C_2 = 3 \times 10^{-3}$) which are nearly symmetric to the nucleus as is illustrated in Fig. 3, showing the C_2 λ4737 Å-profile on January 14, 1974. The ρ^{-1} -law fits relatively well for both C_2 curves, (S) and (RV), indicating a density law $D(\rho) \sim \rho^{-2}$ for the radiating C_2 molecules. On the other hand, the density distribution of Na atoms can be approximated neither by the simple law $D(\rho) \sim \rho^{-2}$, nor by $D(\rho) \sim \rho^{-2}\, e^{-(\rho/\rho_o)}$ (Haser, 1957; Wurm and Balazs, 1963) and should be investigated in more detail. We observe a similar behavior as for Comets Mrkos 1957 V (Greenstein and Arpigny, 1962) and Bennett 1970 II (Rahe et al., 1975).

The intensity evolution of the main emission bands during the period of observation is given in Tables 7 and 8. The intensity values refer to the intensity of the region close to the nucleus (up to about 10^4 km) and are given relative to the brightness of the violet (0-1) band of CN (Table 7) or to that of the (1-2) Swan band of C_2 (Table 8) which are both normalized to 10.0.

The C_2 (1-0) intensity increases relative to the CN (0-1) emission with increasing heliocentric distance (Table 7, r = 0.46 - 0.60 AU). The CO^+ emission, though very faint, decreases relative to CN as the Comet recedes from the sun while the CH emission clearly increases. At r = 0.46 AU the CH lines are still rather weak, but strengthen with growing r

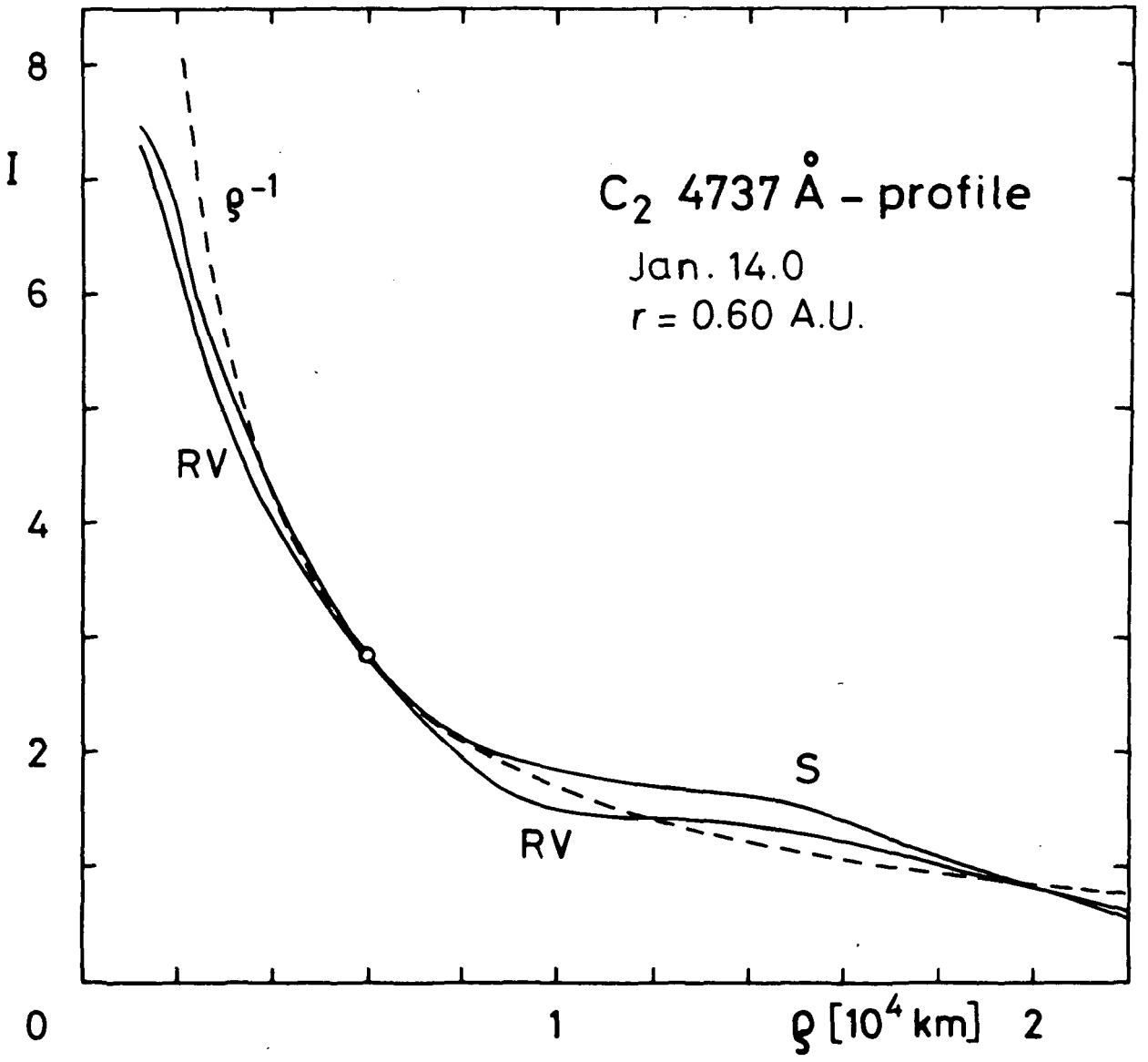

Figure 3: C_2 λ4737 Å-profile as observed on January 14.040 UT, 1974, at r = 0.60 AU. For details see Fig. 1.

Table 7
Intensity as Function of Heliocentric Distance
[relative to CN(0-1) = 10]

Plate No.	Mean air mass	r [A.U.]	C_3 4043.6	C_3 4051.6	CN(0-1) 4214.7	CO^+ 4231	CH 4296.6	CH 4298.0	CH 4303.9	CH 4312.6	CH 4314.2	C_2(1-0) 4737.2
1459	9.4	0.46	-	-	10.0	4.0:	2.7	0.8	1.8	3.6	3.2	18.2
1470	7.6	0.49	5.7	4.6:	10.0	1.7:	2.6	1.5	4.2	4.9	2.4	21.6
1501	5.1	0.60	4.3	8.4	10.0	0.5:	4.1	4.6	8.1	10.7	8.8	33.3

Table 8
Intensity as Function of Heliocentric Distance
[relative to C_2(1-2) = 10]

Plate No.	Mean air mass	r [A.U.]	C_2(1-2) 5585.0	NaI(D_2) 5889.9	NaI(D_1) 5895.9	NH_2 5976.7	[OI] 6300.4	[OI] 6363.9
1436	16 :	0.34	10.0	39.8	27.0	1.8	3.2	-
1439	10.9	0.37	10.0	overexposed		2.7	3.1	0.9
1445	12.0	0.40	10.0	12.3	5.8	-	-	-
1452	9.0	0.43	10.0	32.7	20.2	5.7	-	-
1478	5.9	0.55	10.0	4.1:	-	-	-	-

(see also Fig. 4) . For the first two plates (r = 0.46 and 0.49 AU), the lines 4291 - 4300 Å of the R-branch of the CH ($A^2\Delta - X^2\Pi$) system are weaker than the (0-1) band of CN, in the third spectrum (plate No.1501, r = 0.60 AU) both intensities are comparable. The brightness of the 4312 and 4314 Å emissions of the Q-branch even excels that of the CN (0-1) sequence. The strength of NH_2 also grows as compared to C_2 (1-2) (Table 8, r = 0.34 - 0.55 AU), whereas the intensity of the sodium doublet drops considerably at the same time by about one order of magnitude. It was very strong between January 5 and January 8 at r = 0.34 and r = 0.43 AU, respectively, but had nearly vanished on January 12 at r = 0.55 AU (see also Kohoutek, 1975). However, a pronounced increase in the Na brigthness occured on January 8 at r = 0.43 AU (plate No. 1452). The average intensity ratio of the two sodium D lines was $I(D_2)/I(D_1)$ = 1.7 which is in agreement with the resonance fluorescence hypothesis, according to which this ratio should be $\leqq 2$. It is certainly smaller than the intensity ratio $I(D_2)/I(D_1)$ = 2.5 determined by Warner (1963) from the spectrum of Comet Seki-Lines 1962 III.

The C_3 and the [OI] observations are too limited to allow any conclusion.

The spatial extension of different emissions as function of heliocentric distance can be compared in Table 9. The dimensions are determined along the spectral lines (i.e., their lengths perpendicular to the dispersion) and are clearly limited by exposure time and plate emulsion, thus giving only lower limits of the actual extension of the

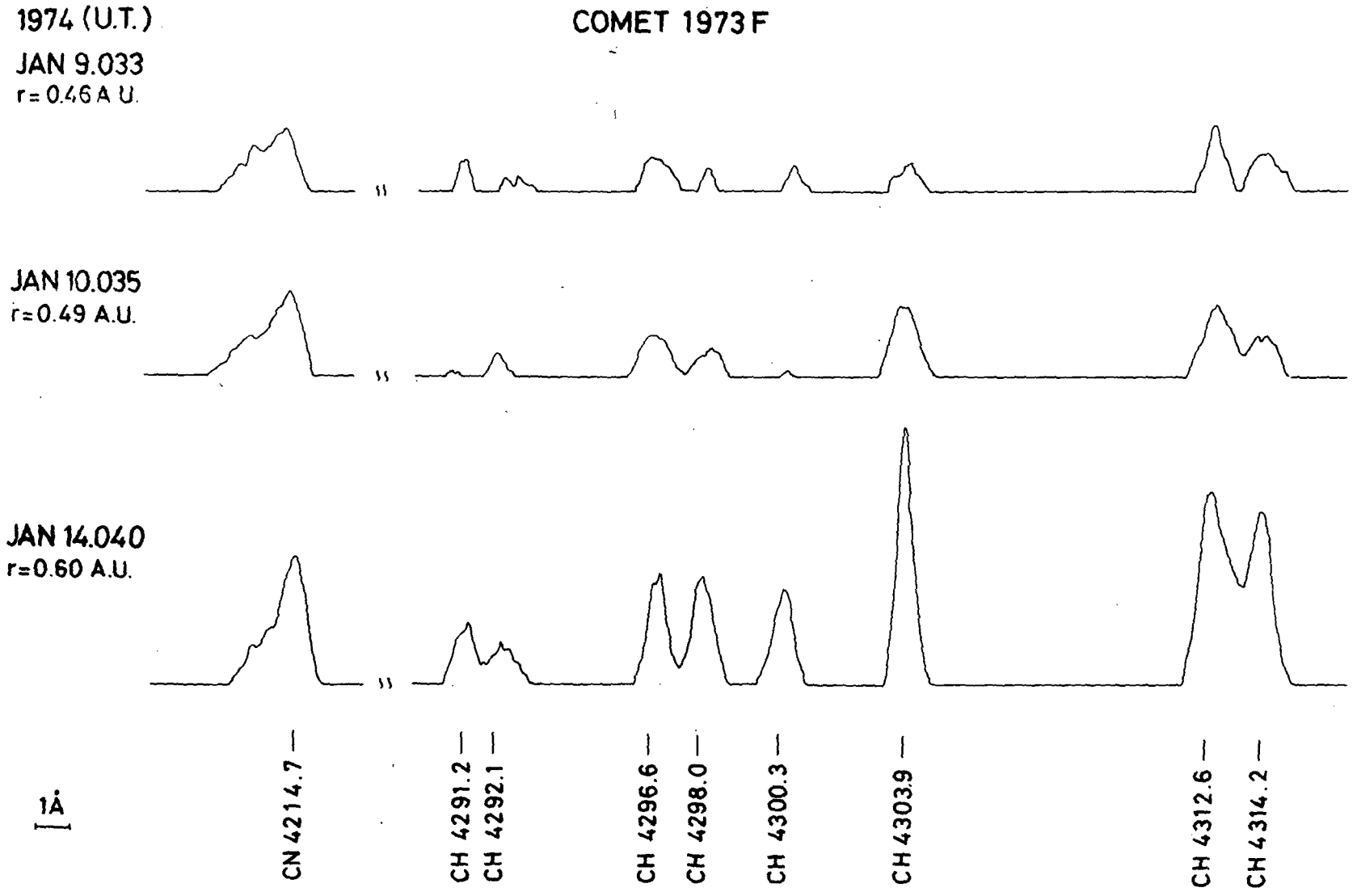

Figure 4: Variation of CH intensity.

Table 9
Extension of Different Emissions (in 10^4 km)

Plate No.	C_2 5165.2	NaI 5889.9	NH_2 5976.7	[OI] 6363.9	CN 3883.4	C_2 4737.1	C_3 4051.6	CH 4312.6
1436	1.68	1.86						
1439	3.89	2.12	0.74	1.43				
1445	2.83	1.27						
1452	2.00	0.87						
1459					2.49	2.70	0.29	0.57
1470					4.80	2.91	0.36	0.69
1501					5.86	4.49	0.23	0.66

various species. Different particles show very different extensions. CN has the greatest extension, C_3 the shortest. Arranged in order of decreasing extension in the head of the Comet we find CN, C_2, CH, C_3. Due to its faintness, the size and shape of the CO^+ emission could not be determined.

The molecular lines are superimposed on a relatively weak continuous spectrum which showed a stronger concentration toward the nucleus than the coma emissions. In Comet 1973f, the continuum (relative to the discrete emissions) was weaker than that of Comets Mrkos 1957 V (Greenstein and Arpigny, 1962) or Bennett 1970 II (Babu and Saxena, 1972) where it was rather strong and the intensity ratio of emissions to continuum small, but it was stronger than that of the "gaseous" Comets Burnham 1960 II (Dossin et al., 1961) or Ikeya 1963 I (Fehrenbach, 1963) where it was very weak and narrow or practically non-existent. This is in agreement with the photometric measurements (Kohoutek, 1975).

We wish to thank Mr. J. Prölss for his assistance with the reduction. We are grateful to the ESO directorate for providing us with observing time at the 1.52 m telescope and to the Stiftung Volkswagenwerk for a grant which supported this work.

References

Babu G.S.D., Saxena P.P., 1972, Bull. Astron. Inst. Czech. 23, 346

Dossin F., Fehrenbach Ch., Haser L., Swings P.,1961, Ann. d'Astrophys. 24, 519

Dressler K., Ramsay D.A., 1959, Phil. Trans. R. Soc. London, A, 251, 553

Fehrenbach Ch., 1963, C.R. Paris 256, 3788

Greenstein J.L., Arpigny C., 1962, Ap. J. 135, 892

Haser L., 1957, Bull. Acad. Roy. Belg. (Classe Sci.), 5th Series, 43, 740

Hunaerts J., 1950, Ann. l'Obs. Roy. Belg., Tome 5, 1

Johnson R.C., 1927, Phil. Trans. R. Soc. London, A, 226, 157

Kohoutek L., 1975, this symposium

Phillips J.G., 1948, Ap. J., 108, 434

Rahe J., McCracken C.W., Donn B., 1975, Astron. Astrophys., in press

Shea J.D., 1927, Phys. Rev. 30, 825

Warner B., 1963, Observatory 83, 223

Weinard J., 1955, Ann. d'Astrophys. 18, 334

Wurm K., Balazs B., 1963, Icarus 2, 334